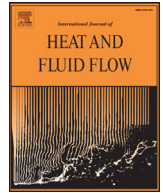




Contents lists available at ScienceDirect

International Journal of Heat and Fluid Flow

journal homepage: www.elsevier.com/locate/ijhff

Near wall dissipation revisited

Sedat Tardu

Laboratoire des Écoulements Géophysiques et Industriels (LEGI) Université Grenoble Alpes Domaine Universitaire CS 40700, 38058 Grenoble Cedex 9, France

ARTICLE INFO

Article history:

Available online xxx

Keywords:

Wall turbulence
 Direct numerical simulations
 Kinetic energy dissipation
 Approximations
 Reynolds number effects
 Stagnation points and dissipation

ABSTRACT

The characteristics of the dissipation of the turbulent kinetic energy in wall-bounded flows are revisited through direct numerical simulations of turbulent channel flows realized in large computational domains up to the Reynolds number $Re_\tau = \frac{h\bar{u}_\tau}{\nu} = 1100$ where \bar{u}_τ is the friction velocity, ν and h stands for the kinematic viscosity and channel half width. It is shown that the local homogeneity assumption is acceptable in the whole layer, while the local isotropy is valid only in the far meso-layer and near the centerline. The mean dissipation in inner scale is Reynolds number dependent in the low-buffer and viscous sub-layers. This is due to the local shear layers induced by the outer-layer irrotational eddies. A conceptual model is subsequently proposed to link the near wall dissipation to the large-scale structures. The dissipation statistics conditioned by fixed amplitudes of the velocity field are also analyzed in order to clarify whether the zero-crossings of the fluctuating velocity components contribute most to the energy dissipation or not. Incidentally, the occurrence of the Eulerian stagnation points is questioned. The largest contribution to the dissipation in the viscous sublayer comes from the level-crossings of the wall normal velocity v component in the spanwise direction, that peaks to 30% when $\nu = 0$. The spanwise direction is the most active in terms of the level-crossing frequencies that are inversely proportional to the corresponding Taylor scales.

© 2017 Elsevier Inc. All rights reserved.

1. Introduction

It is compulsory to conduct a detailed investigation of the dissipation ε_K of the turbulent kinetic energy in wall-bounded flows to improve the turbulence models. The structural complexity of the wall turbulence is coupled with that of the small-scale structures in the direct vicinity of the wall. The fine scale-turbulence is affected by the large-scale inactive motions in the viscous and low buffer sublayers, leading to the Reynolds number dependence of ε_K in this region (Bradshaw 1967; Hoyas and Jiménez 2008; Mathis et al., 2013). The way the large-scales and the finer-scales coupling takes place is one of the most interesting enigmas of the wall turbulence.

Hunt et al. (1987), Hunt and Carruthers (1990) and Hunt and Morrison (2000) argue that the rate of dissipation is controlled by the steepest gradient of the energy containing eddies and should therefore be related to the smallest integral scale. They show that the smallest macro-scale is the integral scale $L_{\nu\nu}^{(x)}$ of the wall normal velocity ν in the streamwise x direction in a turbulent flow with slight shear (SS). They further suppose that $L_{\nu\nu}^{(x)}$ is approximately equal to the dissipation length scale L_{ε_K} defined as $L_{\nu\nu}^{(x)} \approx L_{\varepsilon_K} \equiv \frac{\bar{\nu}^{3/2}}{\varepsilon_K}$. According to these authors, the dissipation of the

kinetic energy ε_K is then approximately invariant with the wall normal distance y and the turbulent intensity $\bar{\nu}^2$ depends on ε_K and y , which, when subjected to dimensional analysis, gives us $\bar{\nu}^2 = C\varepsilon_K^{2/3}y^{2/3}$. The dissipation length scale with SS is therefore a function of $\bar{\nu}^2$ and ε_K leading to $L_{\varepsilon_K}^{-1} \equiv \frac{\varepsilon_K}{(\bar{\nu}^2)^{3/2}} = C^{-3/2}y^{-1} = Ay^{-1}$. However, in a turbulent flow with constant shear *without* the presence of a wall, L_{ε_K} depends on $\bar{\nu}^2$ and on the mean shear i.e. $L_{\varepsilon_K}^{-1} \equiv A' \frac{d\bar{U}/dy}{\bar{\nu}^2}$. The dissipation ε_K is due to the deformation of the small structures by the larger ones, and is controlled by the significant gradients of the structures containing the energy. However, $\varepsilon_K \propto L_{\varepsilon_K}^{-1}$, and consequently the length scale L_{ε_K} near to a real wall depends on the less dominant of the two effects – i.e. on the wall or the shear. Hunt and Morrison (2000) therefore propose to consider the harmonic mean of the two expressions $L_{\varepsilon_K}^{-1} \equiv Ay^{-1} + A' \frac{d\bar{U}/dy}{\bar{\nu}^2}$. This form was evaluated in the analysis based on the rapid distortion theory performed Lee and Hunt (1989). This expression corresponds relatively closely to the DNS data at the start of the outer layer and with low Reynolds numbers, but is not valid next to the wall in the low buffer and viscous sublayers.

Antonia et al. (1991) analyzed the turbulent channel direct numerical simulations data at two low Reynolds numbers $Re_\tau = h^+ = \frac{h\bar{u}_\tau}{\nu} = 180$ and 395 to provide approximate estimations of the kinetic energy dissipation in a wall bounded turbulent flow. Here h is the half-channel width and $(\)^+$ denotes the variables scaled by the

E-mail address: Sedat.Tardu@legi.grenoble-inp.fr

<http://dx.doi.org/10.1016/j.ijheatfluidflow.2017.03.006>
 0142-727X/© 2017 Elsevier Inc. All rights reserved.

kinematic viscosity ν and the shear velocity \bar{u}_τ hereafter. These authors compared the homogeneous, axisymmetric and isotropic approximations with the real dissipation distribution across the channel and analyzed the asymptotic behavior of ε_K at the wall. Their analysis has shown inter alia, that the wall turbulence can be considered locally homogeneous and isotropic only in the far meso-layer and not in the inner layer.

The kinetic energy dissipation reaches its maximum at the wall. Moreover, the Reynolds number dependence of ε_K is concentrated in the low buffer layer and the influence of the large-scale passive eddies on ε_K is accentuated mainly in the viscous sublayer (Hoyas and Jiménez, 2008). Some time ago, Bradshaw (1967) evoked the possibility that the large-scale irrotational eddies can effect the small-scale structures (dissipation) near the wall. The passive structures do not contain vorticity but play the role of outer potential flow. They create local Rayleigh-Stokes shear layers concentrated below the buffer layer and extending over several outer length scale in the streamwise direction. One of the components of the dissipation at the wall is directly related to the turbulent intensity of the wall shear stress that is known to increase slightly with $\ln(Re_\tau)$. Mathis et al. (2013) have shown that the large-scale motions (LSM) induce an amplitude modulation in the instantaneous wall shear stress fluctuations in a way similar to the amplitude modulation felt in the streamwise velocity fluctuations in the buffer layer (Mathis et al., 2009; Marusic et al., 2010).

Kailasnath and Sreenivasan (1993) claim that “the zeros of the velocity signal constitute a part of turbulence dynamics that contributes most to the energy dissipation but nothing at all to the Reynolds stress». It is well established by now that the Liepmann scale based on the zero-crossing frequency of u and the Taylor scale related to $(\partial u/\partial x)^2$ coincide well in wall bounded flows (Sreenivasan et al., 1983; Tardu and Bauer, 2015; Tardu 2016) However, this coincidence does obviously not imply that the dissipation is locally important during the zero-crossings, and this point has not been entirely elucidated.

The aim of this paper is to revisit some of these aspects through the direct numerical simulations (DNS) up to $Re_\tau = 1100$ realized in large computational domains of a fully developed turbulent channel flow. The DNS are briefly detailed in the next section. The validity of the dissipation estimation through local homogeneity, axisymmetry, and local isotropy is subsequently questioned. The effect of the large-scale irrotational eddies on the fine scale turbulence next to the wall is analyzed through a conceptual model. Finally, the conditional contributions to the dissipation of fixed magnitudes of fluctuating velocity components are discussed and different aspects related to this topic are clarified.

2. Direct numerical simulations

Direct numerical simulations (DNS) of four fully developed turbulent channel flows have been performed at $Re_\tau = 180, 395, 590$ and 1100 in particularly large computational domains similarly to Hoyas and Jiménez (2008). Periodical boundary conditions are used in the homogeneous streamwise x and spanwise z directions. The mesh nodes are distributed uniformly along x and z , and refined near the wall in the wall-normal y direction. The mesh size Δy is set to one third of the Kolmogorov scale η near the wall while $\Delta y \approx \eta$ at the centerline. The time integration is performed according to a fractional step approach in which convective and diffusive terms are integrated by a three-stage and third-order low storage Runge-Kutta scheme. High accuracy fourth order optimized explicit schemes using a five-point stencil are used in order to reach spectral-like accuracy. Details can be found in Bauer et al. (2015). The Table 1 recapitulates the simulation characteristics. It is seen that the streamwise and spanwise lengths of the computational domain varies respectively from $L_x = 38h$ to $25h$, and $L_z = 13h$ to $9h$. They are taken particularly large to depict the effect of large-scale outer structures, if any.

The time span used for the statistics is denoted by T in Table 1 and it is also comparable to that used by Hoyas and Jiménez (2008). These authors use short-term averages for the statistical quantities, whereas the procedure chosen here is somewhat different. We first compute the statistical quantities in the homogeneous planes of 10 independent fields. Two fields are considered as independent if they are separated by a time T_p larger than the time required for a particle at the channel center to cross the length of the computational domain in the streamwise direction, i.e. $T_p \geq \frac{L_x}{U_c}$. This means there is at least one large eddy turnover time between two consecutive samples to avoid the interference between the buffer layer coherent structures. Ten independent flow fields yield a total sample of more than 6×10^7 points for $Re_\tau = 1100$ at a given y^+ plane and lead to satisfactory statistical convergence. Note that the criteria of the statistical independence used, is very strict, as most of the wall structures evaluate significantly in time and space within a time period smaller than $\frac{L_x}{U_c}$. Thus, the number of flow fields was increased from ten to N_F within the time span T (last column of Table 1) and their statistical independence was checked.

All of the major turbulence statistics compare perfectly well with published data obtained by pseudo-spectral DNS of the evolution problem for the wall-normal vorticity and the Laplacian of the wall-normal velocity. The DNS data presented here have already been used to analyze different aspects of the wall turbulence in Tardu and Bauer (2015, 2016) and Tardu (2016, 2017).

Table 1

Simulations parameters in the streamwise, wall-normal and spanwise directions (x, y, z). The second column gives the number of computational modes in respectively x, y , and z directions. The resolution in the streamwise, wall-normal and spanwise directions in wall units are provided in columns three to five. Both smallest (first line) and largest (second line) grid spacing are given for wall-normal direction. The number in parenthesis is the wall-normal grid spacing scaled by Kolmogorov length η in the fourth column; L_x and L_z correspond respectively to the size of the computational domain along x and z ; T , and N_F are respectively the time span and the number of flow fields used to compute the statistics.

| Re_τ | $N_x \times N_y \times N_z$ | Δx^+ | Δy^+ | Δz^+ | $\frac{L_x}{h}$ | $\frac{L_z}{h}$ | $\frac{T U_c}{L_x}$ | $\frac{T \bar{u}_\tau}{h}$ | N_F |
|-----------|-------------------------------|--------------|---------------------|--------------|-----------------|-----------------|---------------------|----------------------------|-------|
| 180 | $771 \times 129 \times 387$ | 8.80 | 0.49 (0.31 η) | 5.84 | 12π | 4π | 18 | 40 | 64 |
| | | | 5.59 (1.52 η) | | | | | | |
| 395 | $1691 \times 283 \times 849$ | 8.81 | 0.48 (0.33 η) | 5.85 | 12π | 4π | 12 | 25 | 51 |
| | | | 5.57 (1.26 η) | | | | | | |
| 590 | $1651 \times 423 \times 1113$ | 8.98 | 0.48 (0.34 η) | 5.00 | 8π | 3π | 16 | 19 | 24 |
| | | | 5.56 (1.15 η) | | | | | | |
| 1100 | $3079 \times 789 \times 2075$ | 8.98 | 0.48 (0.34 η) | 5.00 | 8π | 3π | 11 | 13 | 16 |
| | | | 5.55 (0.98 η) | | | | | | |

Download English Version:

<https://daneshyari.com/en/article/7053579>

Download Persian Version:

<https://daneshyari.com/article/7053579>

[Daneshyari.com](https://daneshyari.com)